J. Fluid Mech. (1984), *vol.* 149, *pp.* 161–177
Printed in Great Britain

Sound generation and upstream influence due to instability waves interacting with non-uniform mean flows

By M. E. GOLDSTEIN
National Aeronautics and Space Administration, Lewis Research Center, Cleveland, Ohio 44135

(Received 1 August 1983)

Recent experiments reveal that mean spreading rates of artificially excited shear layers undergo abrupt changes at certain discrete positions within the flow. This paper is concerned with the interaction between externally excited instability waves and these regions of relatively sudden change in mean flow. While the main emphasis is on the acoustic field produced by these interactions, the upstream influence at the nozzle lip is also considered.

1. Introduction

This paper is concerned with the sound produced by artificially excited spatially growing instability waves on subsonic shear layers. These waves would become transcendentally small at transverse infinity if the mean flow were assumed to be parallel, and no acoustic radiation would be produced in that case. But real flows always diverge in the downstream direction and sound can be produced by the interaction of the instability waves with the resulting streamwise variations of the flow. Tam & Morris (1980) treated the mean-flow divergence as a small parameter and used matched asymptotic expansions to calculate the sound generated by this interaction. They concluded that it produces very little sound at subsonic speeds.

Crow & Champagne (1971), Ffowcs Williams & Kempton (1978), and more recently Huerre & Crighton (1983) used Lighthill's (1952) acoustic analogy to calculate the sound produced by this mechanism. These analyses all assume that the shear layer grows in a gradual fashion, but recent experiments of Ho & Huang (1982) and Oster & Wygnanski (1982) reveal that excited shear layers undergo sudden changes in their growth rates at certain discrete locations. Some typical results are shown in figure 1.

Part of the shear-layer growth can probably be attributed to Reynolds stresses produced by the externally excited instability waves (which we identify with the large-scale coherent motions of the flow). The local growth rates of these waves vary with shear-layer thickness and eventually go to zero when the shear layer is sufficiently thick relative to the instability wavelengths. Since the corresponding Reynolds-stress terms will then go to zero, it is not surprising to find that the shear-layer growth rate also goes to zero at this location (or nearly so). What is surprising is that it does so in a very sudden fashion! The shear-layer thickness then remains relatively constant until a lower-frequency (i.e. longer-wavelength) instability wave – usually the first subharmonic of the former – becomes sufficiently large to cause the shear layer to resume its downstream growth. This behaviour is illustrated in figure 2, which is a composite of data taken by Ho & Huang (1982) and Oster & Wygnanski (1982).

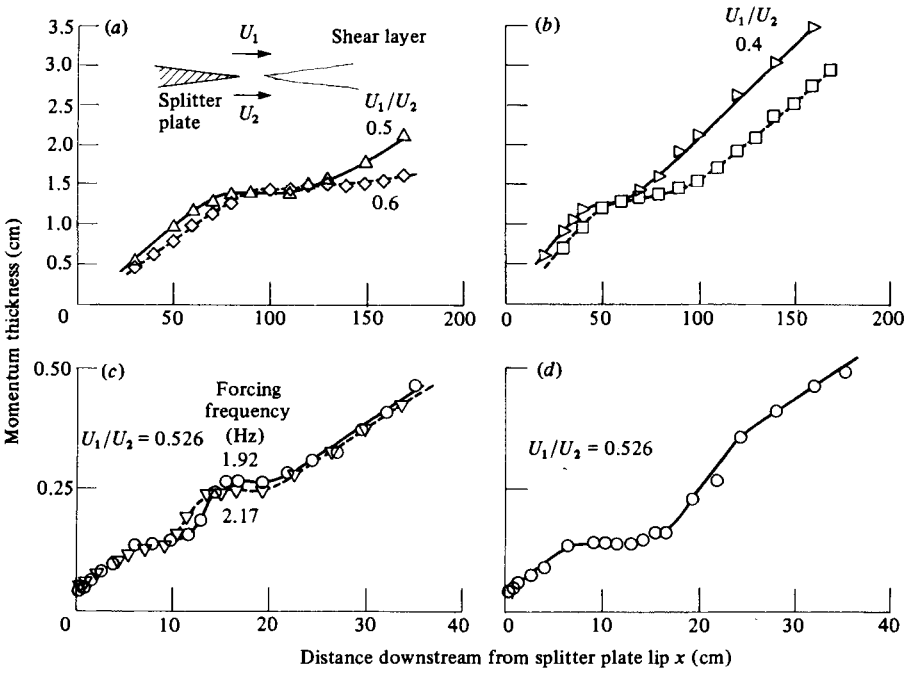

FIGURE 1. Measured spreading rate of forced mixing layer between two parallel streams. (*a*), (*b*) Data of Oster & Wygnanski (1982); forcing frequency 50 Hz, forcing amplitude 0.15 cm. (*c*) Data of Ho & Huang (1982); initial velocity fluctuation approximately 0.1 % of mean. (*d*) Data of Ho & Huang (1982); initial velocity fluctuation 0.07 % of mean; forcing frequency 3.29 Hz.

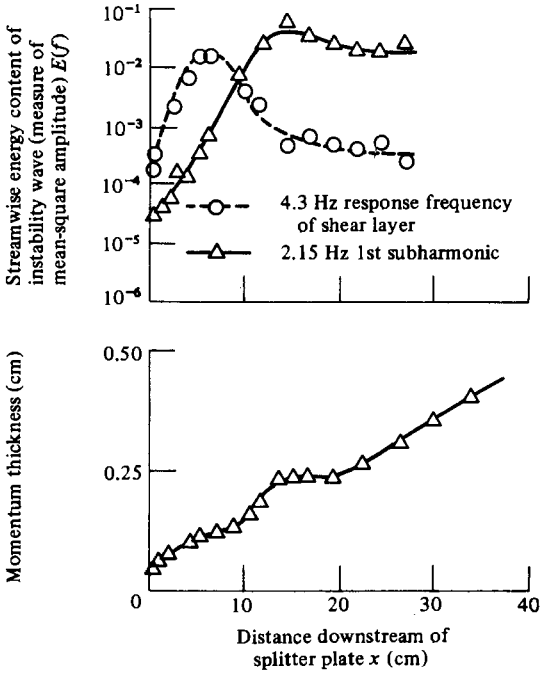

FIGURE 2. Amplification of instability wave an growth of mixing layer. Data of Ho & Huang (1982). Initial velocity fluctuation approximately 0.1 % of mean.

Pressure fluctuations are set up in order to balance the mass and momentum fluctuations that occur when the instability waves pass through these regions of sudden change in shear-layer growth. This paper is concerned with the sound field and 'upstream influence' associated with these fluctuations. The 'upstream influence' or 'feedback' can interact with the splitter-plate lip to produce a downstream-propagating instability wave which could, under certain conditions, be the same instability wave that originally generated the upstream influence. This type of 'resonance' is responsible for producing the so called 'edgetones' that occur when a downstream edge is inserted into a shear layer.

Ho & Huang (1982) detected a significant subharmonic of the excitation frequency near their splitter-plate lip, which they take to be an indication that some sort of feedback mechanism was operative in their experiment. Our analysis shows that the present mechanism is far too weak to produce a feedback loop in their experiment – though it could do so in other experiments.

We are interested in very low-Mach-number flows, so that compressibility effects can only become important over large distances. The shear-layer flow, which is calculated in §2, can then be treated as if it were incompressible. The associated unsteady motion is treated as a linear perturbation about the experimentally observed mean flow. There is now considerable evidence to support the contention that this latter approximation may provide a fairly good description of the real flow even when the amplitude of the unsteady motion is fairly large (relative to the mean). Gaster, Kit & Wygnanski (1984), for example, show that weakly non-parallel stability theory is able to predict the observed transverse distribution of the filtered streamwise velocity fluctuations in two-dimensional shear layers even when the amplitude of the unsteady motion is 20% of the mean velocity. Champagne & Wygnanski (1984) obtain even better agreement for plane wakes, and Strange & Crighton (1983) demonstrated that linear instability theory even works fairly well in the regime where significant nonlinearity is expected to occur. Finally, it is worth noting that the unsteady motion is fairly small relative to the mean in both the Ho & Huang and Oster & Wygnanski experiments because the change in mean velocity (and consequently the instability wave growth rates) are fairly small there.

The mean velocity is assumed to be nearly parallel and slowly varying in the streamwise direction except at the discrete positions (indicated by $S_1, \ldots, S_3$ in figure 3) where it undergoes sudden changes in direction. We treat these locations as 'actuator disks' (Horlock 1978, p. 35) and derive appropriate 'jump conditions' for the unsteady flow in §2.1.

The method of multiple scales is used (Nayfeh 1973, pp. 288 ff.) to calculate the instability waves on the slowly diverging mean flow between the actuator disks. But a 'diffracted' solution, which is constructed in §2.5, must be added to these waves in order to conserve mass and momentum across the disks. This latter solution has an acoustic field which is calculated in §3 by using matched asymptotic expansions to account for compressibility effects.

We first consider the acoustic field produced by a single discontinuity. It behaves like a stationary (i.e. non-convecting) point quadrupole source. This result is then modified to account for interference effects between different discontinuities. The ensuing radiation pattern can be much more directional than those of the individual sources.

Kibens (1980) excited a jet shear layer by using a harmonic acoustic source at the nozzle lip. He found that the jet's natural broadband noise was then suppressed and that most of the sound was radiated at the excitation frequency and its subharmonics.

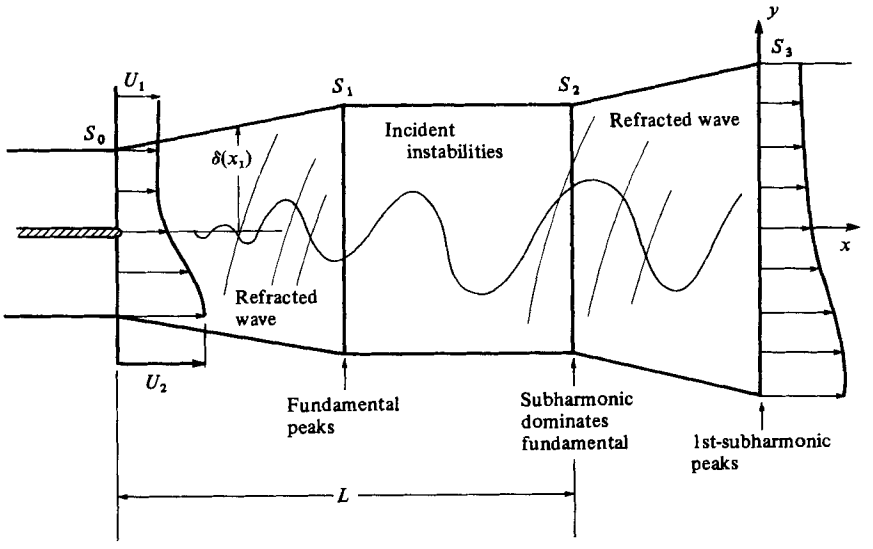

FIGURE 3. Mean-flow configuration.

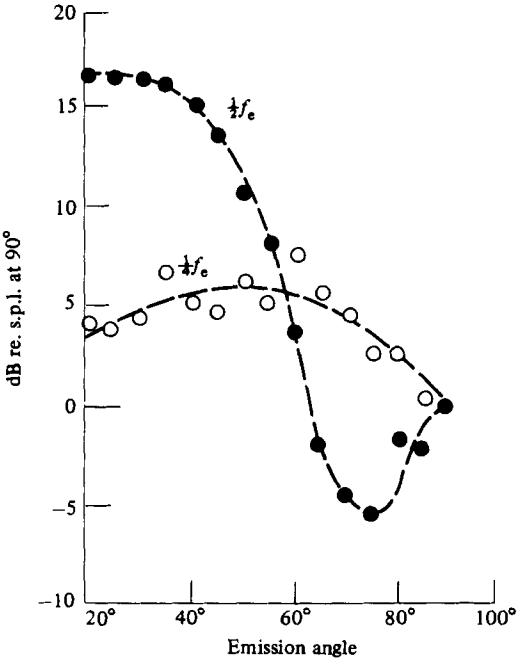

FIGURE 4. Directivity of discrete tones in the enhanced jet. Data from Kim (1983); $f_e \equiv$ excitation frequency; $M = 0.21$. (Directivity pattern at f_e is contaminated by excitation signal.)

His measurements in the near and far fields showed no Doppler shift in frequency – indicating that most of the sound was generated by stationary sources, whose locations he subsequently identified as the vortex-pairing locations. Since the vortex-pairing locations coincide with regions of sudden change in shear-layer growth in the Ho & Huang experiments, the present analysis may be relevant to the pure-tone vortex-pairing noise observed by Kibens (1980).

Laufer & Yen (1983) and Kim (1983) carried out similar experiments – but at much

lower Mach numbers. The former found that all subharmonics of the excitation frequency (the fundamental was contaminated by the excitation signal) radiated much more directionally than the stationary point quadrupole source that would result if interference effects were neglected in the present analysis. But Kim found that the second and higher subharmonics were relatively non-directional in his experiment. (Some of his data are reproduced here as figure 4.) In any case, source-interference effects may be able to explain the observed directionality in Laufer's data, but it does not seem appropriate to make any direct comparison at this stage.

Finally, Zaman (1983) claims that subharmonic tones can only occur when the nozzle boundary layer is laminar. But this is the condition where the instability-wave Reynolds stresses will have the largest effect on shear-layer growth, and consequently where growth-rate discontinuities would be most likely to occur.

The upstream influence is evaluated in §4 and the generation of downstream-propagating instability waves is discussed by using ideas originally proposed by Crighton & Leppington (1974). As already indicated, the resulting instability wave turns out to be much too weak to produce the upstream influence that originally generated this wave in the first place.

2. Flow in the shear layer and near field

The flow in the shear layer will be treated as inviscid and nearly incompressible, but, as will be seen below, first-order terms in the squared Mach number must be retained in order to completely determine the acoustic field produced by this flow. The motion is assumed to be isentropic and the fluid is assumed to be an ideal gas.

2.1. *Formulation*

We suppose that the mean flow, whose configuration is illustrated in figure 3, is two-dimensional and has constant density $\bar{\rho}$. We also suppose that all lengths have been non-dimensionalized by some characteristic thickness of the shear layer, say δ_0, that the velocity has been non-dimensionalized by the average velocity

$$\overline{U} \equiv \tfrac{1}{2}(U_1 + U_2) \tag{2.1}$$

of the two streams, the time t by $\delta_0/\overline{U}$, the density by $\bar{\rho}$ and the pressure by $\bar{\rho}\overline{U}^2$. Finally, we suppose that the mean flow varies only slowly in the streamwise direction, so that

$$U = U(x_1, y), \tag{2.2}$$

$$V = V(x_1, y), \tag{2.3}$$

$$x_1 \equiv \epsilon x, \tag{2.4}$$

where the streamwise and transverse mean-velocity components U and ϵV are $O(1)$ and $O(\epsilon)$ respectively, where ϵ is a small 'spreading' parameter $O(\delta_0/L)$ and L represents some characteristic streamwise distance, say between the nozzle lip and one of the discontinuities in the mean flow.

Now assume that a small-amplitude two-dimensional motion with harmonic time dependence of (non-dimensional) frequency ω is imposed on this mean flow. Then, in the regions between the discontinuities at $S_0, \ldots, S_3$, its streamwise and transverse velocity components $u\,\mathrm{e}^{-\mathrm{i}\omega t}, v\,\mathrm{e}^{-\mathrm{i}\omega t}$ and pressure $p\,\mathrm{e}^{-\mathrm{i}\omega t}$ are determined to $O(\epsilon)$ (and to sufficient accuracy in Mach number) by the linearized momentum and continuity equations

$$\left(-\mathrm{i}\omega + U\frac{\partial}{\partial x}\right)u + v\frac{\partial U}{\partial y} + \frac{\partial p}{\partial x} = -\epsilon\left(V\frac{\partial u}{\partial y} + u\frac{\partial U}{\partial x_1}\right), \tag{2.5}$$

$$\left(-\mathrm{i}\omega+U\frac{\partial}{\partial x}\right)v+\frac{\partial p}{\partial y}=-\epsilon\left(V\frac{\partial v}{\partial y}+v\frac{\partial V}{\partial y}\right), \tag{2.6}$$

$$M^2\left(-\mathrm{i}\omega+U\frac{\partial}{\partial x}\right)p+\frac{\partial u}{\partial x}+\frac{\partial v}{\partial y}=-\epsilon M^2V\frac{\partial p}{\partial y}, \tag{2.7}$$

where M denotes the mean-flow Mach number based on $\bar{U}$ and the (constant) mean-flow sound speed $\bar{C}$. Since the motion is assumed isentropic (and since we are dealing with an ideal gas), conservation of fluctuating mass and momentum requires that u, v and p satisfy the 'actuator-disk' jump conditions (Horlock 1978, p. 35)

$$\text{continuity} \quad \Delta[u+M^2pU]=0, \tag{2.8}$$

$$x\text{-momentum} \quad \Delta[p+2uU+M^2pU^2]=0, \tag{2.9}$$

$$y\text{-momentum} \quad \Delta[Uv+\epsilon(u+M^2pU)\,V]=0, \tag{2.10}$$

across the discontinuities in mean-flow direction, where $\Delta[\ldots]$ denotes a jump in the indicated quantity. It is worth noting that these equations apply to $O(M^2)$, even when the mean density changes by $O(\epsilon)$ across the discontinuities.

2.2. *Similarity variables*

The measurements of Ho & Huang (1982) clearly indicate that the streamwise mean-velocity components can be expressed in similarity form (in the regions between $S_0,\ldots,S_3$)

$$U=U(\eta), \tag{2.11}$$

where

$$\eta\equiv[y-y_0(x_1)]/\delta(x_1), \tag{2.12}$$

$\delta_0\,\delta(x_1)$ is an appropriate local shear-layer thickness, and $\delta_0\,y_0(x_1)$ is the characteristic 'centreline' position of the shear layer.

In order to satisfy continuity, we require that

$$\begin{aligned}V_\perp(\eta,x_1)&\equiv V-(\eta\delta'+y_0')\,U\\&=V_\perp(0,x_1)-\delta'\int_0^\eta U\,\mathrm{d}\eta,\end{aligned} \tag{2.13}$$

where $V_\perp$ is the mean-velocity component in the direction transverse to $\eta=$ constant and the primes denote differentiation with respect to x_1.

Using η and x as new independent variables, we find that the region of flow shown in figure 3 maps into the rectangular region depicted in figure 5 and that (2.5)–(2.7) become

$$\delta\left(-\mathrm{i}\omega+U\frac{\partial}{\partial x}\right)u+vU'+\delta\frac{\partial p}{\partial x}=\epsilon\,[(\eta\delta'+y_0')\,\mathrm{D}(Uu+p)-V\,\mathrm{D}u], \tag{2.14}$$

$$\delta\left(-\mathrm{i}\omega+U\frac{\partial}{\partial x}\right)v+\mathrm{D}p=-\epsilon(V_\perp\,\mathrm{D}v+V'v), \tag{2.15}$$

$$\delta M^2\left(-\mathrm{i}\omega+U\frac{\partial}{\partial x}\right)p+\mathrm{D}v+\delta\frac{\partial u}{\partial x}=\epsilon\,[(\eta\delta'+y_0')\,\mathrm{D}u-M^2V_\perp\,\mathrm{D}p], \tag{2.16}$$

where $\mathrm{D}\equiv\partial/\partial\eta$ and the primes denote total derivatives with respect to the appropriate arguments (i.e. η or x_1).

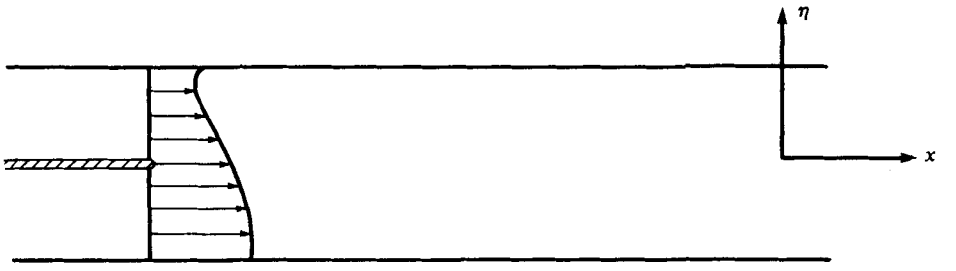

FIGURE 5. Flow configuration in (η, x)-plane.

2.3. *The instability wave*

To lowest order in ϵ, (2.14)–(2.16) are satisfied by the Kelvin–Helmholtz instability wave

$$\{u_0, v_0, p_0\} = \{\bar{u}_0(\eta, x_1), \bar{v}_0(\eta, x_1), \bar{p}_0(\eta, x_1)\}\, \mathrm{e}^{\mathrm{i}\int \alpha(x_1)\,\mathrm{d}x}, \tag{2.17}$$

where $\alpha\delta$ and $\{\bar{u}_0(\eta, x_1), \bar{v}_0(\eta, x_1), \bar{p}_0(\eta, x_1)\}$ represent the eigenvalue and eigenfunction of the compressible Rayleigh equations

$$\mathrm{i}\alpha\delta(U-c)\,\bar{u}_0 + \bar{v}_0\,U' + \mathrm{i}\alpha\delta\bar{p}_0 = 0, \tag{2.18}$$

$$\mathrm{i}\alpha\delta(U-c)\,\bar{v}_0 + \mathrm{D}\bar{p}_0 = 0, \tag{2.19}$$

$$\mathrm{i}\alpha\delta M^2(U-c)\,\bar{p}_0 + \mathrm{D}\bar{v}_0 + \mathrm{i}\alpha\delta\bar{u}_0 = 0, \tag{2.20}$$

corresponding to the boundary condition that

$$\{u_0, \bar{v}_0, \bar{p}_0\} \to 0 \xrightarrow{\text{(exponentially fast)}} \text{as} \quad \eta \to \infty \tag{2.21}$$

and

$$c \equiv \omega/\alpha. \tag{2.22}$$

We suppose that the slowly varying amplitude function, which accounts for mean-flow divergence effects, is incorporated into the definitions of $\bar{u}_0$, $\bar{v}_0$ and $\bar{p}_0$ (which depend on the slow variable x_1). We do not explicitly display it until specific calculations are carried out in §3.

2.4. *The first-order solution*

Since U itself is continuous across $S_1, \ldots, S_3$, it is clear that (2.17) satisfies the jump conditions (2.8)–(2.10) to within an error $O(\epsilon)$. We now extend this solution to include $O(\epsilon)$ terms by putting

$$\{u, v, p\} = \{u_0, v_0, p_0\} + \epsilon\{u_1, v_1, p_1\} + \ldots, \tag{2.23}$$

where $\{u_1, v_1, p_1\}$ satisfies an inhomogeneous system of equations whose inhomogeneous term is calculated from $\{u_0, v_0, p_0\}$.

It is convenient to decompose $\{u_1, v_1, p_1\}$ into the sum of a particular solution that 'eliminates' this inhomogeneous term, but does not satisfy the required jump conditions across $S_1, \ldots, S_3$, and a homogeneous solution $\{u_{\mathrm{H}}, v_{\mathrm{H}}, p_{\mathrm{H}}\}$ that causes these conditions to be satisfied to appropriate order. Thus it follows from (2.14)–(2.16) and (2.17)–(2.20) that

$$\{u_1, v_1, p_1\} = \{\bar{u}_1(\eta, x_1), \bar{v}_1(\eta, x_1), \bar{p}_1(\eta, x_1)\}\, \mathrm{e}^{\mathrm{i}\int \alpha(x_1)\,\mathrm{d}x} + \{u_{\mathrm{H}}, v_{\mathrm{H}}, p_{\mathrm{H}}\}, \tag{2.24}$$

where

$$\mathrm{i}\alpha\delta(U-c)\,\bar{u}_1+\bar{v}_1\,U'+\mathrm{i}\alpha\delta\bar{p}_1=\Big[(\eta\delta'+y_0')\,\mathrm{D}(U\bar{u}_0+\bar{p}_0)-V\,\mathrm{D}\bar{u}_0\Big]-\delta\frac{\partial}{\partial x_1}(U\bar{u}_0+\bar{p}_0), \tag{2.25}$$

$$\mathrm{i}\alpha\delta(U-c)\,\bar{v}_1+\mathrm{D}\bar{p}_1=-(V_\perp\mathrm{D}\bar{v}_0+V'\bar{v}_0)-\delta U\frac{\partial\bar{v}_0}{\partial x_1}, \tag{2.26}$$

$$\mathrm{i}\alpha\delta M^2(U-c)\,\bar{p}_1+\mathrm{D}\bar{v}_1+\mathrm{i}\alpha\delta\bar{u}_1=[(\eta\delta'+y_0')\,\mathrm{D}\bar{u}_0-M^2V_\perp\mathrm{D}\bar{p}_0]-\delta\frac{\partial}{\partial x_1}(\bar{u}_0+M^2U\bar{p}_0); \tag{2.27}$$

$$\delta\Big(-\mathrm{i}\omega+U\frac{\partial}{\partial x}\Big)u_{\mathrm{H}}+v_{\mathrm{H}}\,U'+\delta\frac{\partial p_{\mathrm{H}}}{\partial x}=0, \tag{2.28}$$

$$\delta\Big(-\mathrm{i}\omega+U\frac{\partial}{\partial x}\Big)v_{\mathrm{H}}+\mathrm{D}p_{\mathrm{H}}=0, \tag{2.29}$$

$$\delta M^2\Big(-\mathrm{i}\omega+U\frac{\partial}{\partial x}\Big)p_{\mathrm{H}}+\mathrm{D}v_{\mathrm{H}}+\delta\frac{\partial u_{\mathrm{H}}}{\partial x}=0, \tag{2.30}$$

and it is appropriate to require that $\{\bar{u}_1,\bar{v}_1,\bar{p}_1\}$ satisfy the same boundary condition at infinity as $\{\bar{u}_0,\bar{v}_0,\bar{p}_0\}$.

Inserting (2.23) into (2.8)–(2.10), using (2.17) and (2.24), neglecting terms $O(M^4)$ and equating to zero coefficients of like powers of ϵ, we obtain the following jump conditions for $\{u_{\mathrm{H}},v_{\mathrm{H}},p_{\mathrm{H}}\}$:

$$\text{continuity}\quad \Delta[u_{\mathrm{H}}]=-B\,\Delta[\bar{u}_1], \tag{2.31}$$

$$x\text{-momentum}\quad \Delta[p_{\mathrm{H}}]=-B\,\Delta[\bar{p}_1], \tag{2.32}$$

$$y\text{-momentum}\quad U\,\Delta[v_{\mathrm{H}}]=-B\,\Delta[U\bar{v}_1+V(\bar{u}_0+UM^2\bar{p}_0)], \tag{2.33}$$

where

$$B=\exp\Big(\mathrm{i}\int_{x_0}^{x_{\mathrm{s}}}\alpha(x_1)\,\mathrm{d}x\Big) \tag{2.34}$$

represents the complex 'amplitude' of the instability wave at the position of the discontinuity.

It is worth noting that the right-hand-sides of (2.25)–(2.27) vanish in any region of the shear layer where δ and y_0 remain constant, and we would lose no generality by requiring that $\bar{u}_1\equiv\bar{v}_1\equiv\bar{p}_1\equiv V\equiv 0$ in such regions. The right-hand-sides of the jump conditions (2.31)–(2.32) would then depend only on quantities that come from the variable-δ side of the discontinuity.

2.5. *The diffracted solution*

It is clear that the contributions of each of the discontinuities to the homogeneous solution $\{u_{\mathrm{H}},v_{\mathrm{H}},p_{\mathrm{H}}\}$ are independent of each other to the order of approximation of the analysis. It is therefore necessary to consider only one such discontinuity, which, without loss of generality, we assume to be located at $x=0$. Since the corresponding solution is, to lowest order, defined and continuous everywhere upstream and downstream of $x=0$, and since the coefficients of (2.28)–(2.30) are independent of

x to lowest order, it is convenient to introduce the half-range Fourier transforms

$$\bar{w}_+ \equiv \int_{-\infty}^{0} \mathrm{e}^{-\mathrm{i}kx} w_{\mathrm{H}} \,\mathrm{d}x, \tag{2.35}$$

$$\bar{w}_- \equiv \int_{0}^{\infty} \mathrm{e}^{-\mathrm{i}kx} w_{\mathrm{H}} \,\mathrm{d}x, \tag{2.36}$$

where the symbol w refers to any of the three quantities, u, v, p. Then it follows from (2.28)–(2.30) that

$$\mathrm{i}\delta\Phi\bar{u}_\pm + U'\bar{v}_\pm + \mathrm{i}\delta k\bar{p}_\pm = \mp\delta(Uu_{\mathrm{H}} + p_{\mathrm{H}})|_{x=0\mp}, \tag{2.37}$$

$$\mathrm{i}\delta\Phi\bar{v}_\pm + \mathrm{D}\bar{p}_\pm = \mp\delta U v_{\mathrm{H}}|_{x=0\mp}, \tag{2.38}$$

$$\mathrm{i}\delta M^2\Phi\bar{p}_\pm + \mathrm{D}\bar{v}_\pm + \mathrm{i}\delta k\bar{u}_\pm = \mp\delta(u_{\mathrm{H}} + M^2 U p_{\mathrm{H}})|_{x=0\mp}, \tag{2.39}$$

where

$$\Phi \equiv Uk - \omega \tag{2.40}$$

and $x = 0\mp$ denotes the limit as $x \to 0$ through negative/positive values of x.

Adding the two equations in (2.37), and similarly for the two equations in (2.38) and (2.39), and using (2.31)–(2.33) to eliminate the resulting jumps in $\{u_{\mathrm{H}}, v_{\mathrm{H}}, p_{\mathrm{H}}\}$, yields

$$\mathrm{i}\delta\Phi\bar{u} + U'\bar{v} + \mathrm{i}k\delta\bar{p} = -\delta B\,\Delta[U\bar{u}_1 + \bar{p}_1], \tag{2.41}$$

$$\mathrm{i}\delta\Phi\bar{v} + \mathrm{D}\bar{p} = -\delta B\,\Delta[U\bar{v}_1 + V(\bar{u}_0 + M^2 U\bar{p}_0)], \tag{2.42}$$

$$\mathrm{i}\delta M^2\Phi\bar{p} + \mathrm{D}\bar{v} + \mathrm{i}k\delta\bar{u} = -\delta B\,\Delta[\bar{u}_1 + M^2 U\bar{p}_1], \tag{2.43}$$

where

$$\bar{w} \equiv \bar{w}_+ + \bar{w}_- \tag{2.44}$$

for $w = u$, v or p is the full-range Fourier transform of the indicated quantity.

Eliminating $\bar{u}$ and $\bar{v}$ between these equations yields

$$\Phi^2 \mathrm{L}_0\bar{p} = \frac{\delta B}{\mathrm{i}}\Delta\left[\delta(\omega\bar{u}_1 + k\bar{p}_1 - M^2\Phi U\bar{p}_1) - \mathrm{i}\Phi^2\,\mathrm{D}\left(\frac{U\bar{v}_1 + (\bar{u}_0 + M^2 U\bar{p}_0)\,V}{\Phi^2}\right)\right], \tag{2.45}$$

where

$$\mathrm{L}_0 \equiv \mathrm{D}\frac{1}{\Phi^2}\mathrm{D} - \delta^2\left[\left(\frac{k}{\Phi}\right)^2 - M^2\right] \tag{2.46}$$

is the compressible Rayleigh operator. The right-hand side of (2.45) depends on $\bar{u}_1$, $\bar{v}_1$ and $\bar{p}_1$, which can only be obtained by solving the inhomogeneous systems (2.25)–(2.27), which cannot in general be done analytically. The analysis is only manageable because these quantities can be eliminated from the far-field equations without actually solving (2.25)–(2.27). This is most directly accomplished by rearranging (2.45) to obtain (2.51) below. However, the algebra is quite tedious, and it is easier to work backwards by inserting

$$g_0 \equiv \frac{1}{\alpha\delta}\Delta\left[2V\bar{v}_0 + \frac{1}{\mathrm{i}\alpha\delta}\mathrm{D}\,(A\bar{p}_0)\right], \tag{2.47}$$

$$g_1 \equiv -\frac{\mathrm{i}}{(\alpha\delta)^2}\Delta\left[4V'\bar{v}_0 + \mathrm{D}\left(\bar{\bar{p}}_1 - \frac{\alpha}{\delta}\frac{\partial}{\partial x_1}\left(\frac{\delta\bar{p}_0}{\mathrm{i}\alpha^2}\right) + \frac{2\mathrm{D}A\bar{p}_0}{\mathrm{i}\alpha\delta}\right)\right], \tag{2.48}$$

where

$$\bar{\bar{p}}_1 \equiv \bar{p}_1 - \frac{1}{\delta}\frac{\partial}{\partial x_1}\left(\frac{\delta\bar{p}_0}{\mathrm{i}\alpha}\right) \tag{2.49}$$

and
$$\Lambda \equiv \eta\delta' + y_0', \tag{2.50}$$

into
$$\Phi^3 \mathrm{L}_0\left(\bar{p} - \frac{B\Delta[\bar{\bar{p}}_1]}{\mathrm{i}\alpha\delta}\right) = \frac{\delta B}{\mathrm{i}}\left[\Phi^3 \mathrm{D}\left(\frac{\mathrm{D}g_0 + \mathrm{i}k\delta g_1 - \mathrm{i}M^2c^2\Delta[\Lambda\bar{p}_0]}{\Phi^2}\right) - \delta k^2 g_2 + \mathrm{i}M^2 k g_3\right], \tag{2.51}$$

using (2.18)–(2.20) and (2.25)–(2.27) to rearrange the result, and comparing it with (2.45), to show that
$$g_2 = -\frac{2}{(\alpha\delta)^2}\Delta[U'(V'\bar{v}_0 - V\,\mathrm{D}\bar{v}_0) + cV'\,\mathrm{D}\bar{v}_0] - \frac{1}{\alpha}\Delta\left[\delta\Phi\bar{\bar{p}}_1 + 2c\left(\frac{V'}{\alpha\delta} + \mathrm{i}U'\bar{v}_1\right)\right.$$
$$\left. - 2U'\left(\frac{\partial}{\partial x_1}c + c\frac{\partial}{\partial x_1}\right)\frac{\bar{v}_0}{\alpha}\right] \tag{2.52}$$

and g_3 is a polynomial in k and M. We can calculate the acoustic radiation without knowing anything more about its structure. Together with the third term under the derivative D, it accounts for the compressibility effects on the right-side of (2.51).

Now let F_+ and F_- be the two independent homogeneous solutions of (2.51) that remain bounded as $\eta \to +\infty$ and $\eta \to -\infty$ respectively. Then a particular solution of (2.51) that vanishes as $\eta \to \pm\infty$ is given by
$$\bar{p} = \frac{B\Delta[\bar{\bar{p}}_1]}{\mathrm{i}\alpha\delta} + B\delta\int_{-\infty}^{\infty}\bar{K}(\eta,\tilde{\eta}|k)\sum_{n=0}^{2}(\mathrm{i}k)^n G_n(\tilde{\eta}|k)\,\mathrm{d}\tilde{\eta}, \tag{2.53}$$

where
$$\bar{K}(\eta,\tilde{\eta}) = \frac{F_{\pm}(\tilde{\eta})F_{\mp}(\eta)}{\mathrm{i}\Phi(\tilde{\eta})W(\tilde{\eta})} \quad \text{for} \quad \tilde{\eta} \gtrless \eta, \tag{2.54}$$

$$W \equiv F_-\,\mathrm{D}F_+ - F_+\,\mathrm{D}F_- \tag{2.55}$$

is the Wronskian of $F_\pm$, and
$$G_0 \equiv \Phi^3\,\mathrm{D}\left(\frac{\mathrm{D}g_0 - \mathrm{i}M^2c^2\Delta[\Lambda\bar{p}_0]}{\Phi^2}\right), \tag{2.56}$$

$$G_1 \equiv \delta\Phi^3\,\mathrm{D}\left(\frac{g_1}{\Phi^2}\right) + M^2 g_3, \tag{2.57}$$

$$G_2 \equiv \delta g_2. \tag{2.58}$$

It follows from (2.35), (2.36) and (2.44) that p_{H} is the inverse Fourier transform of (2.53), so that when $x \neq 0$
$$p_{\mathrm{H}} = \frac{B\delta}{2\pi}\sum_{n=0}^{2}\frac{\partial^n}{\partial x^n}\int_{-\infty}^{\infty}\int_{-\infty}^{\infty}\bar{K}(\eta,x|\tilde{\eta})\,G_n(\tilde{\eta}|k)\,\mathrm{e}^{\mathrm{i}kx}\,\mathrm{d}\tilde{\eta}\,\mathrm{d}k, \tag{2.59}$$

where the integration contour for the integration over k is to be taken below the pole at $k = \omega/U$. The contribution from this pole represents the gust or hydrodyamic solution (Goldstein 1979). Since the contour is closed in the lower half-plane when $x < 0$ and in the upper half-plane when $x > 0$, this latter solution only exists downstream of the discontinuity.

Within the shear layer where $\eta = O(1)$, $F_\pm$ possess expansions of the form
$$F_\pm = F_\pm^{(0)} + M^2\delta^2 F_\pm^{(1)} + O(M^4) \quad \text{as} \quad M \to 0, \tag{2.60}$$

where
$$\mathrm{L}_{\mathrm{I}} F_{\pm}^{(0)} = 0, \tag{2.61}$$
$$\mathrm{L}_{\mathrm{I}} F_{\pm}^{(1)} = -F_{\pm}^{(0)}, \tag{2.62}$$
and
$$\mathrm{L}_{\mathrm{I}} \equiv \mathrm{D}\frac{1}{\Phi^2}\mathrm{D} - \left(\frac{k\delta}{\Phi}\right)^2 \tag{2.63}$$

is the incompressible Rayleigh operator. These solutions will vanish at infinity, and in fact satisfy the 'incompressible' boundary conditions

$$F_{\pm}^{(n)} \to \mathrm{e}^{\mp|k|\delta\eta} \quad \text{as} \quad \eta \to \pm\infty, \quad \text{for} \quad n = 0, 1. \tag{2.64}$$

Using the method of variation of parameters, we find that $F_{\pm}^{(1)}$ are given in terms of the zeroth-order solutions by

$$F_{\pm}^{(1)}(\eta) = -F_{\pm}^{(0)} \int^{\eta} \left[\frac{\Phi(\hat{\eta})}{F_{\pm}^{(0)}(\hat{\eta})}\right]^2 \int^{\eta} [F_{\pm}^{(0)}(\tilde{\eta})]^2 \,\mathrm{d}\tilde{\eta}\,\mathrm{d}\hat{\eta}. \tag{2.65}$$

3. The far field

Since the instability waves undergo exponential decay outside the shear layer, the asymptotic behaviour of the flow as

$$r \equiv (x^2 + y^2)^{\frac{1}{2}} \tag{3.1}$$

goes to infinity is primarily determined by the diffracted solution (2.59).

3.1. *Asymptotic form of diffracted solution*

Since, as can be seen from (2.60) and (2.64), $\bar{K} \propto \exp[-|k|\,\delta\,|\eta - \tilde{\eta}|]$ as $|\eta - \tilde{\eta}| \to \infty$, the integral of (2.59) has no point of stationary phase, and the dominant contribution to the integral comes from the region near $k \approx 0$.

The zeroth-order solutions $F_{\pm}^{(0)}$ that satisfy the boundary conditions (2.64) behave like

$$F_{\pm}^{(0)} = \mathrm{e}^{\mp|k|\delta\eta}\left[1 \mp \frac{2k\,|k|\,\delta}{\omega}\int U\,\mathrm{d}\eta + O(k^3)\right] \tag{3.2}$$

uniformly in η as $k \to 0$. Inserting this into (2.65), we find that the first-order solutions are given by

$$F_{\pm}^{(1)} = \pm\frac{F_{\pm}^{(0)}}{2\,|k|\,\delta}\int \{\Phi^2(\tilde{\eta}) - 2k\omega[1 - \mathrm{e}^{\mp 2|k|\delta(\eta-\eta)}]\,U(\tilde{\eta})\}\,\mathrm{d}\tilde{\eta} \tag{3.3}$$

uniformly in η as $k \to 0$.

It follows from (2.12), (2.40), (2.54), (2.55) and (2.60) that

$$\begin{aligned} W &= -2\,|k|\,\delta\left(1 - \frac{2kU}{\omega}\right) + \frac{M^2\delta}{|k|}\Phi^2 + O(k^3, M^2k^2) \\ &= -2\,|k|\,\delta\left(\frac{\Phi}{\omega}\right)^2\left[1 - \frac{1}{2}\left(\frac{M\omega}{k}\right)^2\right] + O(k^4, M^2k^3, M^4) \end{aligned} \tag{3.4}$$

and

$$\begin{aligned} \bar{K} = \frac{\omega^2\left[1 - \dfrac{2\,|k|\,k\delta}{\omega}\left|\displaystyle\int_{\tilde{\eta}}^{\eta} U(\hat{\eta})\,\mathrm{d}\hat{\eta}\right| + \dfrac{M^2\delta^2}{2\,|k|\,\delta}\left|\displaystyle\int_{\eta}^{\tilde{\eta}} \Phi^2(\hat{\eta})\,\mathrm{d}\hat{\eta}\right|\right]\mathrm{e}^{-|k||y-\tilde{y}|}}{2\mathrm{i}\,|k|\,\delta\Phi^3(\tilde{\eta})\,(1 - M^2\omega^2/2k^2)} \\ + O(k^2) + M^2O(k^0) + O(M^4) \end{aligned} \tag{3.5}$$

uniformly in η and $\tilde{\eta}$ as $k, M \to 0$, where $\tilde{y}$ denotes the value of y corresponding to $\tilde{\eta}$, and we have used the fact that W/Φ^2 is equal to a constant. It now follows from (2.55)–(2.59) that terms in g_n that can be expressed as the mth derivative with respect to η of a function that vanishes as $\eta \to \pm\infty$ will make negligible contributions to (2.59) as $r \to \infty$ in comparison with terms that can only be expressed as the $(m-1)$th such derivative. Using (2.18)–(2.20) and (2.25)–(2.27), we find that the second term in square brackets in (2.52) can be expressed as the derivative of a function of this type. Hence inserting (2.47), (2.48) and (2.52) into (2.56)–(2.58), inserting these results and (3.5) into (2.59), integrating by parts, recalling that g_3 is a polynomial in k, and noting that the $O(M^2)$ terms in (2.56) and (2.57) therefore make only negligible contributions, we obtain, upon inverting the Fourier transform (see Lighthill 1964, p. 43),

$$p = \epsilon p_{\mathrm{H}} = \frac{\epsilon B \delta^2(0)}{4}\left[Q_{11}\frac{\partial^2}{\partial x^2} + 2\mathrm{i}Q_{12}\frac{\partial^2}{\partial x\,\partial y} + Q_{22}\frac{\partial^2}{\partial y^2}\right] g(r) + O(r^{-3}) + M^2 O(r^0) + O(M^4) \quad \text{as} \quad r \to \infty, \quad M \to 0, \tag{3.6}$$

where

$$g \equiv \frac{2\mathrm{i}}{\pi}[1 - (\tfrac{1}{2}M\omega r)^2]\ln r \tag{3.7}$$

and

$$Q_{11} = -\frac{2}{(\alpha\delta)^3}\int_{-\infty}^{\infty} \Delta\left[V'\,\mathrm{D}\bar{v}_0 + \frac{U'}{c}(V'\bar{v}_0 - V\,\mathrm{D}\bar{v}_0)\right]\mathrm{d}\eta, \tag{3.8}$$

$$Q_{12} = \frac{2}{(\alpha\delta)^2}\int_{-\infty}^{\infty} \Delta[V'\bar{v}_0]\,\mathrm{d}\eta, \tag{3.9}$$

$$Q_{22} = \frac{2}{(\alpha\delta)}\int_{-\infty}^{\infty} \Delta[V\bar{v}_0]\,\mathrm{d}\eta. \tag{3.10}$$

The incompressible limit is obtained by putting $M = 0$ in (3.7). The result shows that the incompressible pressure fluctuations exhibit quadrupole-type behaviour at large distances from the shear layer. We have retained the $O(M^2)$ terms that exhibit the largest growth rates as $r \to \infty$, since these will be needed in order to determine the acoustic solution completely. It is clear that these terms will not be changed if the instability wave ($\bar{v}_0$ in (3.8)–(3.10)) is treated as incompressible.

3.2. *Evaluation of quadrupole strengths for tanh profile*

Ho & Huang's (1982, see figure 23) measurements indicate that the mean velocity should be well represented by the tanh profile

$$U(\eta) = 1 + \lambda \tanh\eta, \tag{3.11}$$

where (see (2.1))

$$\lambda \equiv \frac{U_1 - U_2}{2\bar{U}}. \tag{3.12}$$

We have already noted that the instability waves achieve their maximum amplitudes at the slope discontinuities S_j, i.e. their neutral-stability points occur at these positions. For example, the fundamental-frequency instability reaches its neutral-stability point at S_1 in figure 3, and, since the shear layer exhibits little or no growth between S_1 and S_2, should remain fairly close to its neutral-stability point until it reaches S_2 – though the data of Ho & Huang (1982) indicates that it actually

undergoes a fair amount of decay† in this region. In any case, most of the fundamental tone should be generated at the slope discontinuity/discontinuities S_j where the fundamental-instability wave achieves its neutral-stability point. This is, of course, also true for the subharmonics.

It is therefore appropriate to treat $\bar{v}_0$ as a neutral-instability wave in (3.8)–(3.10). Fortunately, the neutral eigensolution of the incompressible Rayleigh equation for a tanh profile can be written down in simple closed form (Drazin & Howard 1966, p. 42), viz

$$c = \alpha\delta = 1 \quad \text{and} \quad \bar{v}_0 = A \operatorname{sech} \eta, \tag{3.13), (3.14}$$

where $A = \bar{v}_0(0,0)$ is the slowly varying amplitude function at the position of the discontinuity. Inserting (3.11) into (2.13), inserting the result together with (3.11)–(3.14) into (3.8)–(3.10), and carrying out the indicated integrations, we obtain (Gradshteyn & Ryzhik 1965, pp. 98 and 535)

$$Q_{11} = A\lambda\{\tfrac{1}{3}[\pi + \tfrac{4}{3}\lambda)\,\Delta[\delta'] + \lambda\pi\,\Delta[y_0']\}, \tag{3.15}$$

$$Q_{12} = A\lambda\pi\,\Delta[y_0'], \tag{3.16}$$

$$Q_{22} = A\,2\pi\{\lambda(1-\ln 2)\,\Delta[\delta'] + \Delta[V_\perp(x_1, 0)]\}. \tag{3.17}$$

3.3. *The acoustic solution*

Compressibility effects cannot, of course, be neglected at large distances from the source, even when the Mach number is small – though the mean velocity can be set to zero in this region. The pressure fluctuations due to a harmonic line-monopole source in a non-moving medium is

$$H_0^{(1)}(\omega M r)\,\mathrm{e}^{-\mathrm{i}\omega t}, \tag{3.18}$$

where $H_0^{(1)}$ is the Hankel function in the usual notation. Equation (3.6) suggests that the outer solution should be a superposition of line-quadrupole sources of the form

$$p = \left(q_{11}\frac{\partial^2}{\partial x^2} + 2\mathrm{i}q_{12}\frac{\partial^2}{\partial x\,\partial y} + q_{22}\frac{\partial^2}{\partial y^2}\right) H_0^{(1)}(\omega M r), \tag{3.19}$$

where the quadrupole strengths q_{ij} are determined by matching (in the matched asymptotic expansion sense) with the inner solution given by the former equation.

The one-term outer expansion of the one-term inner expansion of the pressure fluctuations in powers of M^2 (see Van Dyke 1964, p. 64) is given by (3.6) and (3.7) with $M = 0$. Since

$$H_0^{(1)} \to \frac{2\mathrm{i}}{\pi}\ln r \quad \text{as} \quad r \to 0 \quad \text{and} \quad \frac{\partial^2}{\partial x^2}\ln r = -\frac{\partial^2}{\partial y^2}\ln r,$$

it follows that (3.5) and (3.11) will match to lowest order if

$$q_{11} - q_{22} = \tfrac{1}{4}\epsilon B\delta^2(Q_{11} - Q_{22}) \quad \text{and} \quad q_{12} = \frac{\epsilon B\delta^2}{4}Q_{12}. \tag{3.20), (3.21}$$

The individual values of q_{11} and q_{22} are determined by the $O(M^2)$ terms. Thus the outer expansion of the 2-term inner expansion (in power of M^2) produces the term

$$\tfrac{1}{4}\epsilon B\delta^2(Q_{11} + Q_{22})\frac{2\mathrm{i}}{\pi}\ln r.$$

† Which is still relatively small when compared with the growth that it undergoes upstream of the neutral-stability point.

Using the small-argument asymptotic expansion of the Hankel function (Abramowitz & Stegun 1964, p. 360), we find that this term can only be matched by the outer solution if

$$q_{11}+q_{22}=\tfrac{1}{4}\epsilon B\delta^2(Q_{11}+Q_{22}). \tag{3.22}$$

It follows from (3.20)–(3.22) that the far-field pressure fluctuation is also given by (3.6), provided that we replace g by

$$g=H_0^{(1)}(M\omega r). \tag{3.23}$$

Expanding this for large r (Abramowitz & Stegun 1964, p. 364) and inserting the result into (3.6) shows that the far-field pressure fluctuation due to a single mean-slope discontinuity S_j is given by

$$p\sim\frac{\epsilon B\delta^2(0)\,M^2\omega^2}{2(2\pi M\omega r)^{\frac{1}{2}}}\,\mathrm{e}^{\mathrm{i}(M\omega r-\frac{1}{4}\pi)}\,(Q_{11}\cos^2\theta+2\mathrm{i}Q_{12}\cos\theta\sin\theta+Q_{22}\sin^2\theta)+O(M^4)$$
$$\text{as}\quad r\to\infty, \tag{3.24}$$

where $\theta=\cos^{-1}(x/r)$ is the angle that the line connecting the source point S_j and the observation point makes with the x-axis. The Q_{ij} should be reasonably well approximated by (3.15)–(3.17).

Acoustic-interference effects may become significant when the instability wave does not undergo too much decay before reaching the discontinuity downstream of the one where it first saturates. Since Ho & Huang's (1982) measurements suggest that both the shear-layer growth-rate discontinuity and mean-slope discontinuity will be roughly the same at these two locations, we assume that the same is true for the transverse centreline velocity discontinuity $\Delta[V_\perp(x_1,0)]$. Then it would not be unreasonable to assume that Q_{ij} will be equal and opposite at these two locations and that the Bs, which are defined by (2.34), differ only by a factor of $\mathrm{e}^{\mathrm{i}\alpha_0 l}$, where α_0 is the neutral wavenumber of the instability wave and l is the distance between the two discontinuities.

The resulting sound field will then be given by (3.24) multiplied by the interference factor

$$I\equiv 1-\mathrm{e}^{\mathrm{i}\alpha_0 l}$$

when $l\ll 2\pi/M\omega$ and more generally by

$$I=1-\mathrm{e}^{\mathrm{i}\alpha_0 l(1-Mc_0\cos\theta)}, \tag{3.25}$$

where $c_0\equiv\alpha_0/\omega$, when it is not. For a tanh profile (see (3.14)) this becomes

$$I=1-\mathrm{e}^{\mathrm{i}(l/\delta)(1-M\cos\theta)}. \tag{3.26}$$

Interference effects can similarly be accounted for when the instability waves undergo damping between the discontinuities, as they do in Ho & Huang's (1982) experiment, but the exponent in (3.26) will then be complex.

Since the Q_{ij} are effectively real, the mean-squared pressure produced by a single discontinuity is given by

$$\overline{p^2}\sim\frac{(\epsilon|B|\,\delta^2(0)\,M^2\omega^2)^2}{8\pi M\omega r}[(Q_{11}\cos^2\theta+Q_{22}\sin^2\theta)^2+4Q_{12}^2\cos^2\theta\sin^2\theta], \tag{3.27}$$

and by this result multiplied by $|I|^2$ when two discontinuities are involved.

The Q_{ij} should be fairly well approximated by (3.15)–(3.17). These equations show that the acoustic pressure field is the superposition of the fields produced by the

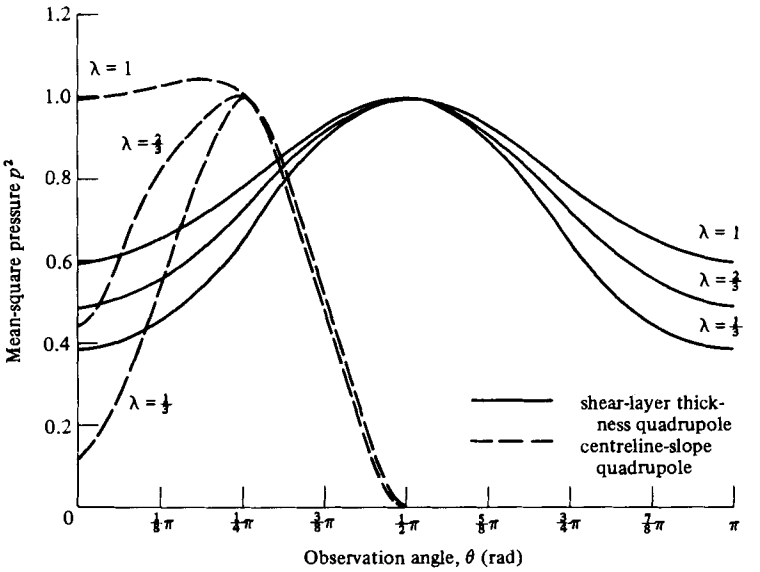

FIGURE 6. Intrinsic radiation patterns produced by shear-layer thickness discontinuity and by shear-layer centreline-slope discontinuity quadrupoles.

shear-layer-thickness discontinuity $\Delta[\delta']$, the centreline-slope discontinuity $\Delta[y_0']$ and the centreline transvere-discontinuity $\Delta[V_\perp(x_1, 0)]$. The basic directivity patterns of the mean-square pressure for the first two of these sources are plotted in figure 6 for $\lambda = \frac{1}{3}, \frac{2}{3}$, and 1. The levels are arbitrary. As is characteristic of fixed point quadrupoles, the results are symmetric about $\theta = \frac{1}{2}\pi$. Only half the $\Delta[y_0']$ pattern is shown. The interference factor $|I|^2$, which we have not included, can substantially modify these patterns, causing them to be highly asymmetric.

4. Upstream influence and feedback

A new flow field will be set up at the surface of the splitter plate in order to cancel the transverse-velocity fluctuation ϵv_H of the diffracted solution at this position, and a new downstream-propagating instability wave will then be produced to eliminate the trailing-edge singularity that would otherwise occur in this flow (Crighton & Leppington 1974; Rienstra 1981). As noted in §1, the process can be self-sustaining, i.e. resonant, when the latter instability wave coincides with the one that originally produced the diffracted solution. But this can only occur if ϵV_H and $\bar{v}_0(0, x)$, the original instability-wave amplitude, are roughly equal at the trailing edge.

Since this point lies far upstream (in terms of shear-layer thicknesses δ) of the discontinuity where ϵv_H was originally generated, the corresponding pressure fluctuation ϵp_H is well approximated by (3.6) with g given by (3.7) (with M set equal to zero) when compressibility is not important and by (3.23) when it is. The Mach number is low enough so that it is unimportant in the Ho & Huang (1982) experiment, and high enough so that it probably is important in the Oster & Wygnanski (1982) experiment.

We only consider the incompressible case. Then since $|x| \gg |y|$ it follows from (2.29) and (3.6) that

$$\epsilon v_H \sim \frac{\epsilon B \delta^2(0)}{2\omega} Q_{12} \frac{\partial^3}{\partial x \partial y^2} g = -\frac{2i\epsilon B}{\omega \delta(0) \pi} \left[\frac{\delta(0)}{x}\right]^3 Q_{12}. \tag{4.1}$$

For a tanh profile (3.13) and (3.126) imply that

$$\frac{\epsilon v_{\mathrm{H}}}{|\bar{v}_0(0,x)|} \sim -2i\epsilon\sigma\lambda\left[\frac{\delta(0)}{x}\right]^3 \Delta[y_0'] \tag{4.2}$$

at the location x of the splinter plate, where (see (2.34) and the equation following (3.15))

$$\sigma \equiv \frac{AB}{|\bar{v}_0(0,x)|} \tag{4.3}$$

is the total amplification of the centreline transverse-velocity fluctuation of the instability wave, i.e. the ratio of the maximum to minimum values of this quantity. Although Ho & Huang (1982) did not measure σ explicitly, we expect it to be of the same magnitude as the square root of their 'streamwise energy content' $E(f)$ (in their notation). The ratios of maximum to minimum $E^{\frac{1}{2}}$ are never much more than 10^2 in their experiment, which is consistent with the predictions of linear stability theory for their flow.

Although Ho & Huang (1982) present no results for the physical centreline slope discontinuity $\epsilon\Delta[y_0']$, they did measure this quantity, and Professor Ho was kind enough to send me the results, which show that this quantity never exceeds 5×10^{-2}. λ was about $\frac{1}{3}$ in their experiment, and we estimate that $\delta(0)/x$, where $\delta_0\,\delta(0)$ is roughly twice the momentum thickness, was about 3×10^{-2}. These estimates imply that $\epsilon v_{\mathrm{H}}/|\bar{v}_0(0,x)|$ was always very small ($\sim 10^{-4}$) at the end of the spltter plate in the Ho & Huang (1982) experiment, so that the present mechanism could not have produced a resonant interaction in this case.

I would like to thank Professor C. M. Ho of the University of Southern California and Professor R. E. Arndt of the University of Minnesota for sending me some of their unpublished data.

REFERENCES

Abramowitz, M. & Stegun, I. A. 1964 *Handbook of Mathematical Functions*. National Bureau of Standards.

Champagne, F. & Wygnanski, I. 1984 Submitted to *J. Fluid Mech.*

Crighton, D. G. 1981 *J. Fluid Mech.* **106**, 261.

Crighton, D. G. & Leppington, F. G. 1974 *J. Fluid Mech.* **64**, 393.

Crow, S. C. & Champagne, F. H. 1971 *J. Fluid Mech.* **48**, 547.

Drazin, P. G. & Howard, H. N. 1966 *Adv. Appl. Mech.* **9**, 1.

Ffowcs Williams, J. E. & Kempton, A. J. 1978 *J. Fluid Mech.* **84**, 673.

Gaster, M., Kite, E. & Wygnanski, I. 1984 Large-scale structures in a forced turbulent mixing layer. Submitted to *J. Fluid Mech.*

Goldstein, M. E. 1979 *J. Fluid Mech.* **91**, 601.

Gradshteyn, I. S. & Ryzhik, I. M. 1965 *Tables of Integrals, Series, and Products*. Academic.

Ho, C. M. & Huang, L.-S. 1982 *J. Fluid Mech.* **119**, 443.

Horlock, J. H. 1978 *Actuator Disk Theory*. McGraw-Hill.

Huerre, P. & Crighton, D. G. 1983 Sound generation by instability waves in a low Mach number flow. *AIAA 8th Aeroacoustics Conf., Paper* 83-0661.

Kibens, V. 1980 *AIAA J.* **18**, 434.

Kim, H. 1983 Noise from acoustically excited jets. Ph.D. thesis, University of Minnesota, St Anthony Falls Hydraulics Laboratory (to be published).

LAUFER, J. & YEN, T.-C. 1983 Nature of the acoustic sources in a low Mach number jet. *AIAA 8th Aeroacoustics Conf., Paper* 83-0660.

LIGHTHILL, M. J. 1952 *Proc. R. Soc. Lond.* **A211**, 564.

LIGHTHILL, M. J. 1964 *An Introduction to Fourier Analysis and Generalized Functions.* Cambridge University Press.

NAYFEH, A. H. 1973 *Perturbation Methods.* Wiley.

OSTER, D. & WYGNANSKI, I. 1982 *J. Fluid Mech.* **123**, 91.

RIENSTRA, S. W. 1981 *J. Fluid Mech.* **108**, 443.

STRANGE, P. J. R. & CRIGHTON, D. G. 1983 *J. Fluid Mech.* **139**, 231.

TAM, C. K. W. & MORRIS, P. J. 1980 *J. Fluid Mech.* **98**, 349.

VAN DYKE, M. 1964 *Perturbation Methods in Fluid Mechanics.* Academic.

ZAMAN, K. B. M. Q. 1983 Large scale coherent structure and far-field jet noise. *Presented at 4th Turbulent Shear Flow Conf., Karlsruhe,* 12–14 *September.*